

# Mechanism of the Reduction of an Oxidized Glutathione Peroxidase Mimic with Thiols

Gavin S. Heverly-Coulson and Russell J. Boyd\*

Department of Chemistry, Dalhousie University, Halifax, Nova Scotia, Canada B3H 4R2

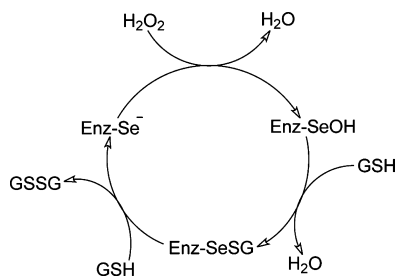
**S** Supporting Information

**ABSTRACT:** *N,N*-dimethylbenzylamine-2-selenol is a well-known, efficient glutathione peroxidase mimic. This compound reduces peroxides through a three-step catalytic mechanism, of which the first step has been well-characterized computationally. The mechanism for the reaction of *N,N*-dimethylbenzylamine-2-selenenic acid with a thiol, the second step in the catalytic cycle, is studied using reliable electronic structure techniques. Two different mechanisms are identified, using either a thiol or a deprotonated thiolate as the nucleophile. It is found that the lowest energy barrier mechanism incorporates two explicit solvent molecules to shuttle the thiol hydrogen to the leaving hydroxyl group, while the alternative mechanism using the thiolate has a barrier four times higher.

## 1. INTRODUCTION

The glutathione peroxidase (GPx) family of selenoenzymes<sup>1</sup> plays an important role in the human body's antioxidant system as efficient reducers of hydroperoxides. The selenium moiety in GPx has been identified as the amino acid selenocysteine, the selenium analogue of cysteine,<sup>2</sup> and it is well-established that it is the active group within the enzyme.<sup>2–4</sup> Both experiments<sup>3</sup> and computer modeling<sup>5</sup> have provided a good understanding of the GPx enzymatic cycle. It follows a three-step pathway, outlined in Scheme 1, with a deprotonated selenolate anion

**Scheme 1. Proposed Catalytic Cycle for the Reduction of Hydrogen Peroxide by GPx**

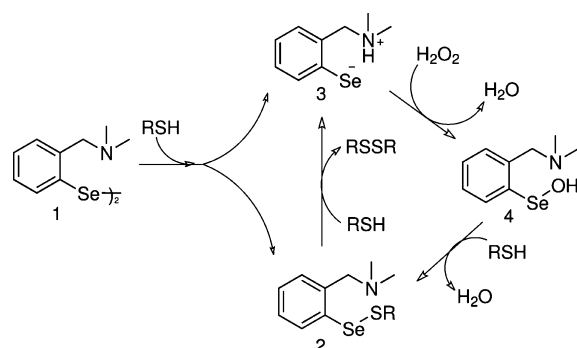


reducing a peroxide to water, forming a selenenic acid in the first step. In the second step, a thiol reacts with the selenenic acid, liberating water and forming a selenylsulfide. In the final step, a second thiol reduces the selenylsulfide bond back to a selenol and produces a disulfide.

Deficiencies in the GPx system can lead to oxidative stress, which can have negative effects on proteins, lipids, DNA, and cell membranes. The use of small organoselenium compounds that mimic the behavior of GPx has been proposed for treatment of conditions such as stroke and acute inflammation, which have been tied to increased reactive oxygen species concentrations. The first such compound, ebselen (2-phenyl-1,2-benzisoselenazol-3(2*H*)-one),<sup>6,7</sup> was proposed nearly 30 years ago. Although ebselen has never seen use as a

pharmaceutical (positive results were seen in a phase II clinical trial for treatment of ischemic stroke victims with ebselen;<sup>8</sup> however, its low solubility and catalytic activity have prevented it from seeing further use), it has prompted the proposal of a wide variety of GPx mimics.<sup>9–20</sup> Of the GPx mimics proposed, *N,N*-dimethylbenzylamine-2-selenol (DMBS)<sup>10</sup> has received much attention over the past two decades, due in part to its high GPx-like activity *in vitro*. The generally accepted catalytic cycle, shown in Scheme 2 for this antioxidant, which follows a

**Scheme 2. Proposed Catalytic Cycle for the Reduction of Hydrogen Peroxide by DMBS**



mechanism similar to GPx, was proposed by Iwaoka and Tomoda.<sup>21</sup> To the best of our knowledge, there has been no report of a complete computational study of the reactions in the DMBS catalytic cycle. We have previously reported on the peroxide reduction step of the cycle.<sup>22,23</sup>

In experimental studies using DMBS as a catalyst for the reaction of hydrogen peroxide with a thiol, the first proposed catalytic intermediate, a selenenic acid, is not observed, instead

**Special Issue:** Berny Schlegel Festschrift

**Received:** July 20, 2012

a rapid conversion of the selenol to a selenylsulfide is seen. This implies that the intermediate between these two species is short-lived and is quickly converted to the selenylsulfide. Iwaoka and Tomoda<sup>21</sup> assigned a selenenic acid structure to this intermediate through spectroscopic observations after reacting DMBS with hydrogen peroxide without any thiol present to continue the reaction. They also observed the higher oxoacids (seleninic and selenonic acids) in their reaction mixtures. Regardless of the relative ratios of the three oxoacids, after adding a thiol, all the acids are rapidly converted to the selenylsulfide. Similar behavior is found for GPx, where the seleninic acid form has been observed through crystallographic methods.<sup>3</sup>

The instability and high reactivity of selenenic acids has long been known. In solution they often react to form seleninic acids and diselenides. Some of the first stable selenenic acids reported were later proven to be selenenic acid anhydrides.<sup>24,25</sup> Throughout the 1980s, various stable phenyl-selenenic acids were reported, mostly stabilized by coordination with ortho electron withdrawing groups, such as esters<sup>26</sup> and nitro groups.<sup>27</sup> Others have used bulky alkyl groups, as in 2,4,6-tri-*tert*-butylphenyl selenenic acid, to stabilize the selenenic acid group.<sup>28</sup> It was not until 1997 that a stable selenenic acid was characterized as a crystal rather than in solution. This was accomplished by burying the selenenic acid moiety in the conical cavity of *p*-*tert*-butylcalix[6]arene.<sup>29</sup> Although the surrounding calixarene prevented the formation of diselenides or anhydrides of this species, other common reactions of selenenic acids, such as with peroxide to form the seleninic acid or thiol to produce the selenylsulfide, were still observed.

In spite of the reaction of a selenenic acid with thiol being well-known in the literature, this reaction has received little attention by computational chemists. In a density-functional theory (DFT) study of the complete enzymatic cycle of GPx, the Morokuma group<sup>5</sup> found that the oxidized selenocysteine reacts with ethanethiol via a one-step reaction with synchronous transfer of the S–H hydrogen to the leaving hydroxyl group and formation of the Se–S bond. A DFT study of the catalytic cycle of GPx mimics,<sup>30</sup> using benzeneselenenic acid and hydrogen sulfide, found a mechanism very similar to the one found by the Morokuma group. In this model, the barrier for this reaction is predicted to be 68 kJ/mol.

In this work, we present a study of the mechanism of the selenenic acid substitution step for the DMBS catalytic cycle. Multiple potential mechanisms are modeled using modern electronic structure theory methods and compared through geometric and energetic parameters to determine which is most favorable.

## 2. COMPUTATIONAL METHODS

All calculations were performed with the Gaussian 09<sup>31</sup> suite of programs. Geometry optimizations were performed using the B3PW91 hybrid DFT functional, composed of Becke's three-parameter exchange functional (B3)<sup>32</sup> and Perdew and Wang's correlation functional (PW91)<sup>33</sup> with the 6-31+G(d,p) Pople basis set, as suggested by the benchmarks we previously performed.<sup>34,35</sup> Transition states were found with Schlegel's synchronous transit-guided quasi-Newton (STQN) method,<sup>36,37</sup> and the reaction path was followed using intrinsic reaction coordinate (IRC)<sup>38,39</sup> calculations. Frequency calculations were performed on all optimized structures at the same level of theory to confirm whether the structure is a local minimum or first-order saddle point and to obtain

thermochemical corrections. Accurate energies were obtained for all systems at the B3PW91/6-311+G(2df,p) level. Solvent effects for an aqueous (dielectric constant of 78.3553) or methanolic (dielectric constant of 32.613) environment were included in all calculations using the conductor-like polarizable continuum model (CPCM). Cartesian coordinates for all systems studied are given in Tables S1–S4.

The topology of the electron density was studied using quantum theory of atoms in molecules (QTAIM)<sup>40,41</sup> calculations performed using AIMAll (Version 12.06.03).<sup>42</sup>

## 3. RESULTS AND DISCUSSION

In this document, all energy barriers are given as the difference between the transition state (TS) and reactant complex (RC)

**Scheme 3. Schematic Outline of the Reaction of a Thiolate with the Selenenic Acid of DMBS**

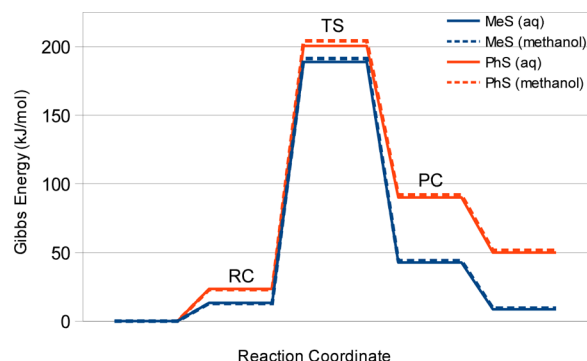
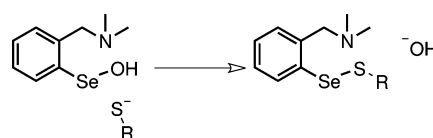
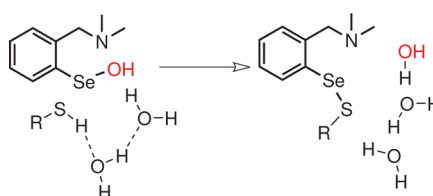


**Figure 1.** Reaction profile for the reaction of a thiolate with the selenenic acid of DMBS. Energies calculated in an aqueous solvent are shown with a solid line and those in a methanolic solvent with a dashed line.

**Table 1. Reaction Energies for Nucleophilic Attack of Various Thiols on the Selenenic Acid of DMBS, in kJ/mol**

nucleophile	solvent	$\Delta G^\ddagger$	$\Delta G_{\text{rxn}}$
MeS <sup>−</sup>	water	175.4	29.3
MeS <sup>−</sup>	methanol	178.5	31.2
PhS <sup>−</sup>	water	177.0	66.7
PhS <sup>−</sup>	methanol	181.2	67.0
MeSH	water	49.1	−76.3
PhSH	water	43.0	−66.1

**Scheme 4. Solvent-Assisted Nucleophilic Attack of a Thiol on the Selenenic Acid of DMBS**



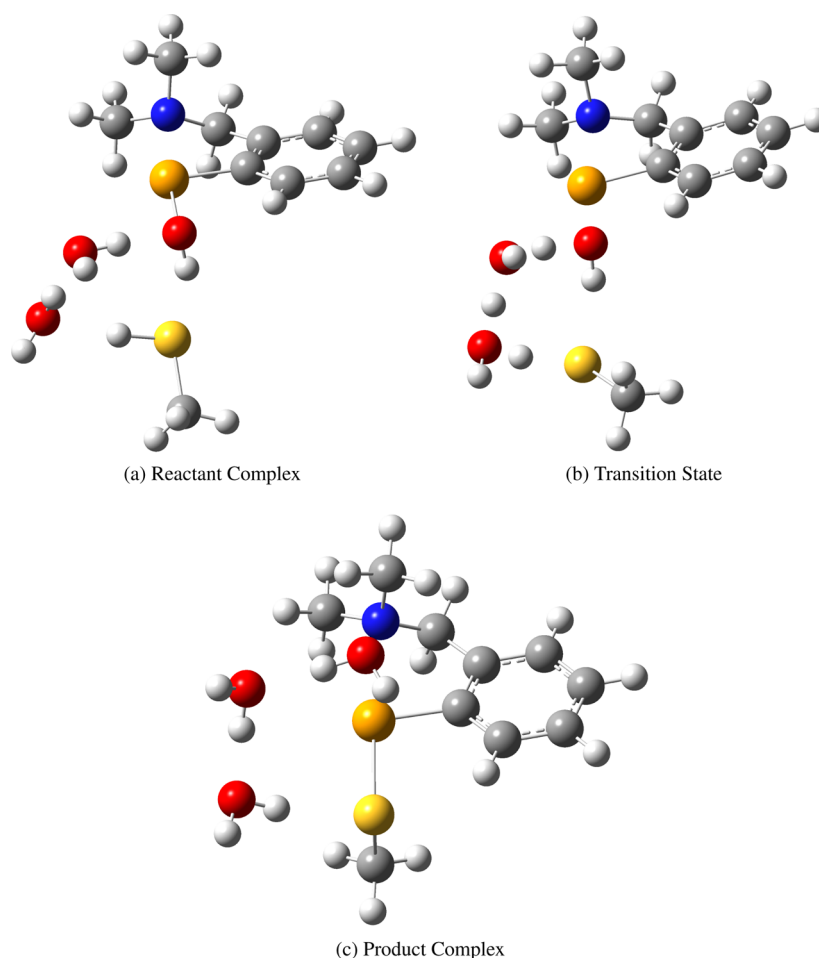


**Figure 2.** Structures found for the water-assisted reaction of methanethiol with the selenenic acid of DMBS.

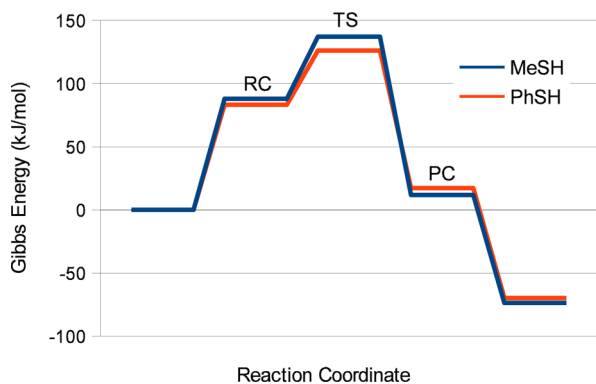


**Figure 3.** Reaction profile for the reaction of a thiol with the selenenic acid of DMBS assisted by two water molecules.

energies. We chose to present the energies in this way for a number of reasons because although the Gibbs energy of the reactant complexes are higher than the infinitely separated reactants, this is not the case for enthalpies, where the formation of the RC is favored, indicating that the high Gibbs energy of the RC is primarily an effect of entropy. If the concentrations of the reactants in solution are sufficiently high, they would overcome the entropic barrier and form the RC.

If the thiol is deprotonated, a highly nucleophilic thiolate can attack the selenium center of the selenenic acid. Using this nucleophile, the expected reaction would be nucleophilic attack

of the thiolate at the selenium center with a hydroxide ion as the leaving group, outlined schematically in Scheme 3.

The reaction described was modeled using the thiolates of methanethiol and thiophenol. The predicted reaction profiles are shown in Figure 1. Modeling their reaction with the selenenic acid of DMBS in water predicts energy barriers of 175.4 and 177.0 kJ/mol, respectively. An aqueous environment would be found *in vivo*; however, many of the *in vitro* studies of GPx mimics are conducted in methanolic environments. Modeling this reaction with methanol as the solvent increases the energy barriers slightly to 178.5 and 181.2 kJ/mol for the thiolates of methanethiol and thiophenol, respectively.

Although the energy barriers do not change significantly with the use of methanethiol or thiophenol, the total energy of reaction is quite different between the two (Table 1). With both solvents and thiolates, the reaction is endergonic, by about 30 kJ/mol for the alkylthiol and double that for the arylthiol. The large difference in stability of the products may be due to differences in the selenylsulfides produced. The Se–S bond is 0.04 Å longer with thiophenol than methanethiol, indicating a weaker, less stable bond. There will be significant steric repulsion between the two phenyl rings, which sit perpendicular to each other, whereas the methyl group is significantly smaller and will have little interaction with the phenyl ring in DMBS.

Experimental studies have found that this step of the DMBS catalytic cycle is very fast; in some studies, the researchers were unable to observe selenenic acid at all. Knowing this, it is

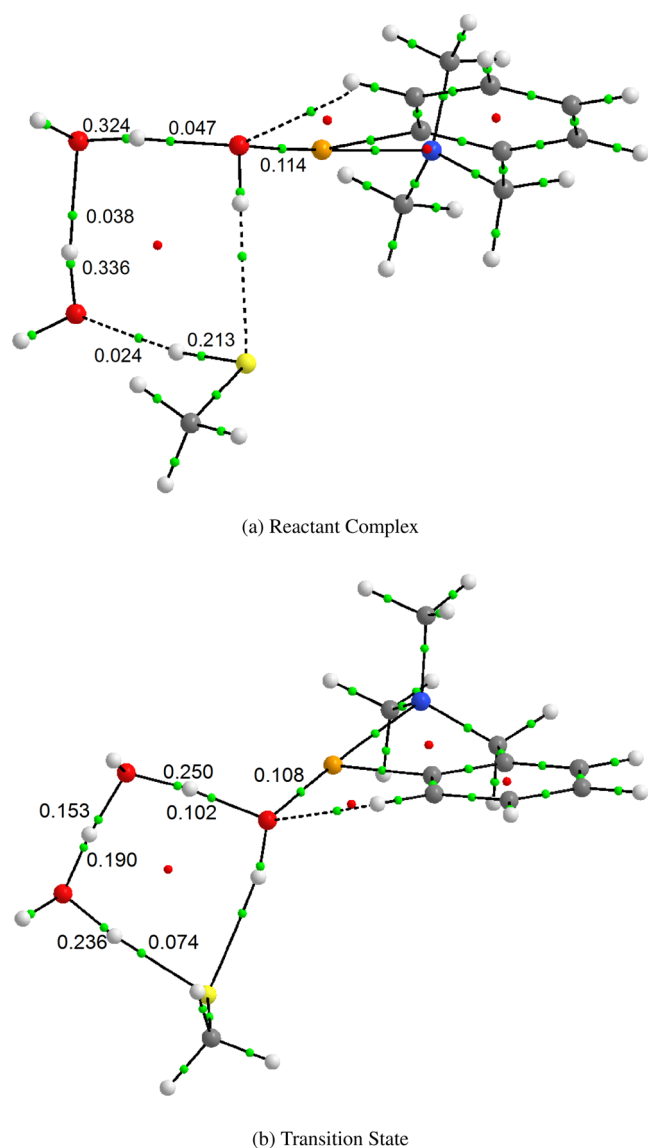


**Figure 4.** Molecular graphs of the water-assisted reaction of methanethiol with the selenenic acid of DMBS. Bond and ring critical points are denoted by green and red spheres, respectively. Bond critical point densities given in atomic units.

unlikely that the reaction proceeds via nucleophilic attack of a thiolate. This reaction is predicted not only to have very large energy barriers but also to be endergonic by up to 67 kJ/mol. Much of this is likely due to the hydroxide ion, which is a very poor leaving group. If a neutral thiol is used instead, water could be formed as the leaving group, which is more favorable.

In their modeling of the GPx mechanism, the Morokuma group<sup>5</sup> found a concerted transfer of the thiol hydrogen to the leaving hydroxyl group with formation of the Se–S bond. This results in a four-centered transition state (TS) that is likely to be under a lot of strain. Additionally, in the reactant complex (RC), it is more favorable for the hydroxyl group to donate a hydrogen bond to the sulfur than for the thiol to donate a bond to the oxygen. In the GPx active site, this is overcome through a nearby glutamine residue that accepts a hydrogen bond from the hydroxyl to the carbonyl in its side chain, allowing the incoming thiol to hydrogen bond to the oxygen. However, there are no such groups in DMBS to facilitate this type of interaction, so it is unlikely that such a complex would be

formed. Instead, if the reaction is performed in a protic solvent, solvent molecules could be used as a proton shuttle, transferring the thiol hydrogen to the hydroxyl group through a chain of solvent molecules. A reaction of this type is outlined schematically in Scheme 4.

Attempts were made to follow the reaction of the selenenic acid of DMBS with methanethiol both with and without explicit solvent molecules. As expected, without solvent molecules, a reactant complex forms with the hydroxyl group hydrogen bonded to the sulfur in the thiol. With this arrangement of the atoms, there is no way to transfer the thiol hydrogen to the hydroxyl group. To facilitate this, solvent molecules were added to the reactant complex to act as a proton shuttle. A single water molecule does not have enough flexibility to accept a hydrogen bond from the thiol and also donate a hydrogen bond to the hydroxyl group. Therefore, a single water molecule will not be effective as a proton shuttle. The addition of a second water molecule forms a chain in the reactant complex that accepts a hydrogen bond from the thiol and donates to the hydroxyl (see Figure 2a). The transition state shows a concerted transfer of three protons (from thiol to water, water to water, and water to hydroxyl) with a lengthening of the Se–O bond (see Figure 2b). Following the reaction path around the transition state, using IRC, shows that the hydrogens are transferred in a “cascade” mechanism, with the thiol hydrogen transferred first, followed by the water-to-water transfer, and finally the water-to-hydroxyl transfer.

The concerted reaction, using two water molecules as a proton shuttle, has a reasonably low energy barrier shown in the reaction profile in Figure 3, varying slightly depending on the thiol used. If methanethiol is used, the energy barrier is 49.1 kJ/mol, while the barrier for thiophenol is 43.0 kJ/mol. The slightly lower barrier with thiophenol is likely due to its lower  $pK_a$ .<sup>43</sup> These barriers are roughly a quarter of those found for the same reaction using the thiolate. Additionally, they are about the same as found for the preceding peroxide reduction step of this reaction,<sup>22</sup> which is in agreement with experimental kinetic studies that indicate that these two steps proceed quickly. Unlike when using thiolates, the reaction of a thiol with the selenenic acid of DMBS is exergonic by about 65–75 kJ/mol, demonstrating the increased stability of water as a leaving group compared to a hydroxide ion.

The QTAIM molecular graphs for the reactant complex (RC) and transition state (TS) of the solvent-assisted reaction mechanism are shown in Figure 4. These can be used to learn more about the proton transfers in this mechanism by comparing the electron densities at the bond critical points in the RC and TS. The QTAIM results agree well with mechanism observed through IRC. In the transition state, the first proton transfer (from the thiol to a water) is nearly complete, with  $\rho_{O-H}$  of 0.236 au (note that  $\rho_{O-H}$  for the O–H bonds not participating in the proton transfer are about 0.36 au). The second proton transfer (from water to water) is about half complete with  $\rho_{O-H}$  of 0.190 and 0.153 au for the bonds breaking and forming, respectively. The final proton transfer (from water to the acid hydroxyl) has only just begun with  $\rho_{O-H}$  of 0.250 and 0.102 au for the water and hydroxyl oxygens, respectively. Complete QTAIM bond critical point data are given in Tables S5 and S6.

#### 4. CONCLUSIONS

Two mechanisms for the reaction of the selenenic acid of DMBS with a thiol have been modeled, using either a highly



nucleophilic thiolate or a more moderate thiol. It is found that the use of a thiol is more favorable than the thiolate.

With a thiolate as the nucleophile, the energy barrier for this reaction is around 175 kJ/mol. This barrier is much higher than expected for this reaction, since it is observed to proceed very quickly. Additionally, the reaction is predicted to be endergonic by 31 or 67 kJ/mol for the thiolates of methanethiol and thiophenol, respectively. Both the high barrier and endergonic products are related to the leaving group in this mechanism, a hydroxide ion. Hydroxide is a poor leaving group, so there will be a high barrier associated with breaking the Se–O bond and it will be less stable than the reactants.

An alternative mechanism uses a thiol as the nucleophile. In this mechanism, the hydrogen on the sulfur is transferred to the hydroxyl of the selenenic acid, making water the leaving group. This proton transfer does not occur directly but instead makes use of two molecules of water from the surrounding solvent as a proton shuttle. This mechanism has a low energy barrier of 49 and 43 kJ/mol for methanethiol and thiophenol, respectively. It is also exergonic overall, by 76 and 66 kJ/mol for methanethiol and thiophenol, respectively, easily making this mechanism more favorable than the one using thiolates.

## ■ ASSOCIATED CONTENT

### ● Supporting Information

Cartesian coordinates for all systems studied and QTAIM bond critical point data for water-assisted mechanisms. This material is available free of charge via the Internet at <http://pubs.acs.org>.

## ■ AUTHOR INFORMATION

### Corresponding Author

\*E-mail: [Russell.Boyd@dal.ca](mailto:Russell.Boyd@dal.ca).

### Notes

The authors declare no competing financial interest.

## ■ ACKNOWLEDGMENTS

We gratefully acknowledge the Natural Sciences and Engineering Research Council of Canada (NSERC) for financial support. Computational facilities are provided by ACEnet, the regional high performance computing consortium for universities in Atlantic Canada. ACEnet is funded by the Canada Foundation for Innovation (CFI), the Atlantic Canada Opportunities Agency (ACOA), and the provinces of Newfoundland and Labrador, Nova Scotia, and New Brunswick.

## ■ REFERENCES

- (1) Rotruck, J. T.; Pope, A. L.; Ganther, H. E.; Swanson, A. B.; Hafeman, D. G.; Hoekstra, W. G. *Science* **1973**, *179*, 588–590.
- (2) Forstrom, J. W.; Zakowski, J. J.; Tappel, A. L. *Biochemistry* **1978**, *17*, 2639–2644.
- (3) Epp, O.; Ladenstein, R.; Wendel, A. *Eur. J. Biochem.* **1983**, *133*, 51–69.
- (4) Rocher, C.; Lallanne, J.; Chaudière, J. *Eur. J. Biochem.* **1992**, *205*, 955–960.
- (5) Prabhakar, R.; Vreven, T.; Morokuma, K.; Musaev, D. G. *Biochemistry* **2005**, *44*, 11864–11871.
- (6) Müller, A.; Cadenas, A.; Graf, P.; Sies, H. *Biochem. Pharmacol.* **1984**, *33*, 3235–3239.
- (7) Wendel, A.; Fausel, M.; Safayhi, H.; Tiegs, G. *Biochem. Pharmacol.* **1984**, *33*, 3241–3245.
- (8) Yamaguchi, T.; Sano, K.; Takakura, K.; Saito, I.; Shinohara, Y.; Asano, T.; Yasuhara, H. *Stroke* **1998**, *29*, 12–17.
- (9) Reich, H. J.; Jasperse, C. P. *J. Am. Chem. Soc.* **1987**, *109*, 5549–5551.
- (10) Wilson, S. R.; Zucker, P. A.; Huang, R.-R. C.; Spector, A. J. *Am. Chem. Soc.* **1989**, *111*, 5936–5939.
- (11) Jacquemin, P. V.; Christiaens, L. E.; Renson, M. J. *Tetrahedron Lett.* **1992**, *33*, 3863–3866.
- (12) Galet, V.; Bernier, J.-L.; Henichart, J.-P.; Lesieur, D.; Abadie, C.; Rochette, L.; Lindenbaum, A.; Chalas, J.; de la Faverie, J.-F. *R. J. Med. Chem.* **1994**, *37*, 2903–2911.
- (13) Back, T. G.; Dyck, B. P. *J. Am. Chem. Soc.* **1997**, *119*, 2079–2083.
- (14) Mughesh, G.; Panda, A.; Singh, H. B.; Puneekar, N. S.; Butcher, R. J. *Chem. Commun.* **1998**, 2227–2228.
- (15) Wirth, T. *Molecules* **1998**, *3*, 164–166.
- (16) Erdelmeier, I.; Tailhan-Lomont, C.; Yadan, J.-C. *J. Org. Chem.* **2000**, *65*, 8152–8157.
- (17) Mughesh, G.; Panda, A.; Singh, H. B.; Puneekar, N. S.; Butcher, R. J. *J. Am. Chem. Soc.* **2001**, *123*, 839–850.
- (18) Back, T. G.; Moussa, Z. *J. Am. Chem. Soc.* **2003**, *125*, 13455–13460.
- (19) Back, T. G.; Moussa, Z.; Parvez, M. *Angew. Chem., Int. Ed.* **2004**, *43*, 1268–1270.
- (20) Sarma, B. K.; Manna, D.; Minoura, M.; Mughesh, G. *J. Am. Chem. Soc.* **2010**, *132*, 5364–5374.
- (21) Iwaoka, M.; Tomoda, S. *J. Am. Chem. Soc.* **1994**, *116*, 2557–2561.
- (22) Heverly-Coulson, G. S.; Boyd, R. J. *J. Phys. Chem. A* **2010**, *114*, 1996–2000.
- (23) Heverly-Coulson, G. S.; Boyd, R. J. *J. Phys. Chem. A* **2010**, *114*, 10706–10711.
- (24) Reich, H. J.; Willis, W. W.; Wollowitz, S. *Tetrahedron Lett.* **1982**, *23*, 3319–3322.
- (25) Kice, J. L.; McAfee, F.; Slebocka-Tilk, H. *Tetrahedron Lett.* **1982**, *23*, 3323–3326.
- (26) Reich, H. J.; Hoeger, C. A.; Willis, W. W. *J. Am. Chem. Soc.* **1982**, *104*, 2936–2937.
- (27) Kang, S. I.; Kice, J. L. *J. Org. Chem.* **1986**, *51*, 295–301.
- (28) Reich, H. J.; Jasperse, C. P. *J. Org. Chem.* **1988**, *53*, 2389–2390.
- (29) Saiki, T.; Goto, K.; Okazaki, R. *Angew. Chem., Int. Ed.* **1997**, *36*, 2223–2224.
- (30) Benkova, Z.; Kóna, J.; Gann, G.; Fabian, W. M. F. *Int. J. Quantum Chem.* **2002**, *90*, 555–565.
- (31) Frisch, M. J.; Trucks, G. W.; Schlegel, H. B.; Scuseria, G. E.; Robb, M. A.; Cheeseman, J. R.; Scalmani, G.; V. Barone, B. M.; Petersson, G. A.; Nakatsuji, H.; Caricato, M.; Li, X.; Hratchian, H. P.; Izmaylov, A. F.; Bloino, J.; Zheng, G.; Sonnenberg, J. L.; Hada, M.; Ehara, M.; Toyota, K.; Fukuda, R.; Hasegawa, J.; Ishida, M.; Nakajima, T.; Honda, Y.; Kitao, O.; Nakai, H.; Vreven, T.; J. A. Montgomery, J.; Peralta, J. E.; Ogliaro, F.; Bearpark, M.; Heyd, J. J.; Brothers, E.; Kudin, K. N.; Staroverov, V. N.; Kobayashi, R.; Normand, J.; Raghavachari, K.; Rendell, A.; Burant, J. C.; Iyengar, S. S.; Tomasi, J.; Cossi, M.; Rega, N.; Millam, J. M.; Klene, M.; Knox, J. E.; Cross, J. B.; Bakken, V.; Adamo, C.; Jaramillo, J.; Gomperts, R.; Stratmann, R. E.; Yazyev, O.; Austin, A. J.; Cammi, R.; Pomelli, C.; Ochterski, J. W.; Martin, R. L.; Morokuma, K.; Zakrzewski, V. G.; Voth, G. A.; Salvador, P.; Dannenberg, J. J.; Dapprich, S.; Daniels, A. D.; Farkas, O.; Foresman, J. B.; Ortiz, J. V.; Cioslowski, J.; Fox, D. J. *Gaussian 09*, Revision A.02; Gaussian, Inc.: Wallingford, CT, 2009.
- (32) Becke, A. D. *J. Chem. Phys.* **1993**, *98*, 1372–1377.
- (33) Perdew, J. P.; Wang, Y. *Phys. Rev. B* **1992**, *45*, 13244–13249.
- (34) Pearson, J. K.; Ban, F.; Boyd, R. J. *J. Phys. Chem. A* **2005**, *109*, 10373–10379.
- (35) Heverly-Coulson, G. S.; Boyd, R. J. *J. Phys. Chem. A* **2011**, *115*, 4827–4831.
- (36) Peng, C.; Schlegel, H. B. *Isr. J. Chem.* **1993**, *33*, 449–454.
- (37) Peng, C.; Ayala, P.; Schlegel, H. B.; Frisch, M. J. *Comput. Chem.* **1996**, *17*, 49–56.
- (38) Gonzalez, C.; Schlegel, H. B. *J. Chem. Phys.* **1989**, *90*, 2154–2161.
- (39) Gonzalez, C.; Schlegel, H. B. *J. Phys. Chem.* **1990**, *94*, 5523–5527.

- (40) Bader, R. F. W. *Atoms in Molecules—A Quantum Theory*; Oxford University Press: Oxford, 1990.
- (41) *The Quantum Theory of Atoms in Molecules: From Solid State to DNA and Drug Design*; Matta, C. F., Boyd, R. J., Eds.; Wiley-VCH: Weinheim, 2007.
- (42) Keith, T. A. *AIMAll*, Version 12.06.03, 2012. Available online: [aim.tkgristmill.com](http://aim.tkgristmill.com).
- (43) Danehy, J. P.; Noel, C. J. *J. Am. Chem. Soc.* **1960**, 82, 2511–2515.